The KASCADE view of cosmic rays

K. Bernlöhr[a], T. Antoni[a], W. D. Apel[a], F. Badea[b], K. Bekk[a], E. Bollmann[a], H. Bozdog[b], I. M. Brancus[b], A. Chilingarian[c], K. Daumiller[d], P. Doll[a], J. Engler[a], F. Feßler[a], H. J. Gils[a], R. Glasstetter[d], R. Haeusler[a], W. Hafemann[a], A. Haungs[a], D. Heck[a], T. Holst[a], J. R. Hörandel[d,*], K.-H. Kampert[a,d], J. Kempa[e], H. O. Klages[a], J. Knapp[d,†], H. J. Mathes[a], H. J. Mayer[a], J. Milke[a], D. Mühlenberg[a], J. Oehlschläger[a], M. Petcu[b], H. Rebel[a], M. Risse[a], M. Roth[a], G. Schatz[a], F. K. Schmidt[d], T. Thouw[a], H. Ulrich[a], A. Vardanyan[c], B. Vulpescu[b], J. H. Weber[d], J. Wentz[a], T. Wibig[e], T. Wiegert[a], D. Wochele[a], J. Wochele[a], J. Zabierowski[f], S. Zagromski[a]

(The KASCADE Collaboration)

[a] Institut für Kernphysik, Forschungszentrum Karlsruhe, 76021 Karlsruhe, Germany
[b] National Institute of Physics and Nuclear Engineering, 7690 Bucharest, Romania
[c] Cosmic Ray Division, Yerevan Physics Institute, Yerevan 36, Armenia
[d] Institut für Experimentelle Kernphysik, University of Karlsruhe, 76021 Karlsruhe, Germany
[e] Department of Experimental Physics, University of Lodz, 90950 Lodz, Poland
[f] Soltan Institute for Nuclear Studies, 90950 Lodz, Poland

1. Introduction

Although cosmic rays are known for almost 90 years and the extensive air showers (EAS) initiated by cosmic rays of energies of the order of 10^{15} eV (1 PeV) and more are known for more than 60 years now, their origin remains a puzzle. Even the most prominent feature in the cosmic ray spectrum, the *knee* at an energy of several PeV, is known for 40 years and still not really understood – not due to a lack of theories but because accurate measurements are extremely difficult. At flux levels below 1 particle per square meter and year, direct measurements from satellites and balloons are still impracticable. At the knee and beyond ground-based EAS experiments prevail. Among the present major EAS experiments, the KArlsruhe Shower Core and Array DEtector (KASCADE) experiment [1,2] is quite unique in being fully designed for measuring the composition of cosmic rays in the energy region around the knee.

One of the important aspects in the design is to measure not just a single composition-sensitive EAS observable but as many as possible. There are several reasons for that. First, primary cosmic ray particles and their energies cannot be directly measured but can only be inferred by comparing measured observables with those expected from simulations. Interaction models used in these simulations (e.g. with the CORSIKA program [3]) have improved over time but remaining systematics are still a concern. The systematics are mainly a consequence of the largely unexplored forward region in hadron-hadron interactions at collider energies and also of the extrapolation in centre-of-mass energies beyond present colliders. The interaction models may also contain approximations not understood well enough. Systematics in different models show up in different ways in the various observables which can be often disentangled from the a-priori unknown composition. Second, different observables are correlated but not redundant. Combining several observables can well improve the mass separation and the energy estimation. Third, systematics in the experimental analysis are easier to assess with independent observables.

*Present address: University of Chicago, Enrico Fermi Institute, Chicago, IL 60637.
†Now at: University of Leeds, Leeds LS2 9JT, U.K.

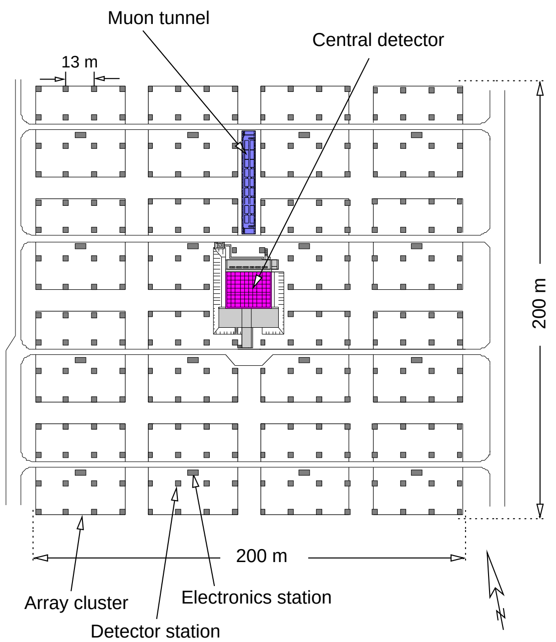

Figure 1. The KASCADE experiment near Karlsruhe. The array of 252 detector stations is subdivided into 16 clusters, each with a dedicated electronics station for data readout.

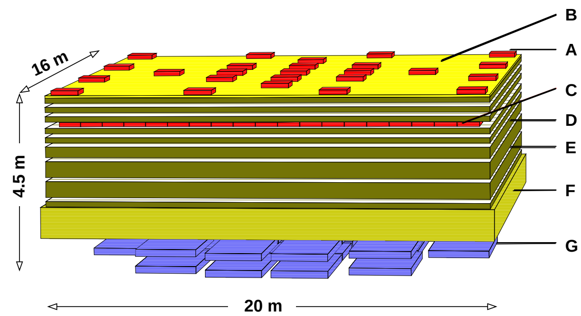

Figure 2. The central detector of the KASCADE experiment. A: top cluster, B: 5 cm lead, C: trigger layer, D: iron, E: TMS chambers, F: concrete, G: MWPC.

2. The KASCADE experiment

KASCADE is located near Karlsruhe, Germany, at an altitude of 110 m a.s.l. It consists of three main components: the *array*, the *muon tunnel*, and the *central detector*.

The array covers an area of about 200×200 m^2 (see Figure 1) with 252 detector stations instrumented with scintillation counters. Two different types of counters are used. Two to four e-γ detectors per station with 5 cm high liquid scintillators of 0.79 m^2 area are each viewed by one photomultiplier (PM). Below 10 cm of lead and 4 cm of iron, the muon detector of 3.24 m^2 with four quadrants of 3 cm thick plastic scintillator is viewed, via 12 wavelength shifter bars, by a total of 4 PMs. For each station the signal sum and the earliest time are recorded, separately for e-γ and muon detectors. The inner 4 of 16 array clusters are not instrumented with muon detectors but with four instead of two e-γ detectors each.

The muon tunnel with an area of 5.4×48 m is, to a large extent, covered with three horizontal layers of streamer tubes and vertical layers at both side walls. The installation is not fully complete at this time but will be finished in 1999.

The central detector (see Figure 2) is a more complex instrument. The main instrument is a 16×20 m^2 hadron calorimeter [4] with 4000 tons of iron as absorber material. It has 8 layers fully instrumented with room-temperature liquid ionisation chambers filled with tetramethylsilane (TMS). With a segmentation of 25×25 cm a total of 40 000 readout channels are used. Thanks to the fine segmentation, tracks of single hadrons above about 50 GeV energy can be reconstructed by the hadronic showers initiated in the calorimeter. Up to several hundred hadrons can be found near the cores of large showers. Readout of the calorimeter is triggered by a *trigger layer* with 456 scintillation counters which are also used as muon counters. Readout may also be triggered by the array.

On top of the central detector, the *top cluster* of 50 scintillation counters mainly measures the density and time-of-arrival of electrons. The measurement of e-γ energy deposition is now being extended by an additional 9$^{\text{th}}$ calorimeter layer between the top cluster and the 5 cm of lead absorber, above the iron stack. Below the calorimeter, two layers of *multiwire proportional chambers* (MWPC, 122 m^2 sensitive area each) are used as position and direction sensitive muon counters, with a threshold energy above 2 GeV. To improve the muon coverage below the calorimeter, an additional layer of streamer tubes is now being installed.

Due to the different detectors, KASCADE is able to reconstruct a large number of shower observables. These include, among others, from the array the shower direction, core position, electron number N_e and *truncated muon number* $N_\mu^{\rm tr}$ (which is integrated over the 40–200 m core distance range). From the MWPCs the number of reconstructed muons and numbers characterising their hit pattern, like the multi-fractal dimensions D_6 and D_{-6}, are obtained. From the calorimeter, the number of reconstructed hadrons $N_{\rm h}$, the total hadronic energy $E_{\rm h}$ seen and that of the most energetic hadron are obtained, as well as a number of other parameters. The trigger layer also provides numbers of hadrons and muons as well as individual muon arrival times.

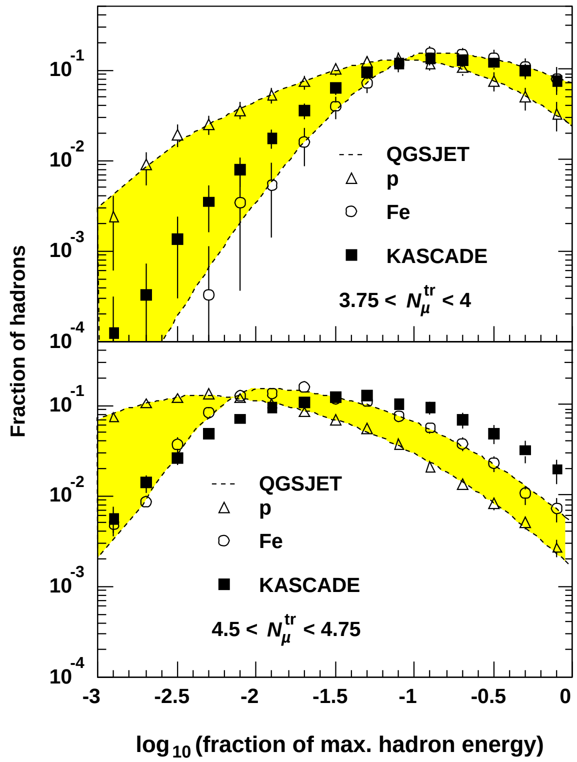

Figure 3. Interaction model test with QGSJET (proton and iron primaries) compared to KASCADE measured data. Shown are the distributions of individual hadrons having a given fraction of the most energetic hadron, for two different $N_\mu^{\rm tr}$ intervals, corresponding to primary energies of about 2 and 12 PeV, respectively. The shaded bands indicate the allowed regions in simulations, for arbitrary cosmic ray composition.

3. Interaction model tests

The air shower simulation program CORSIKA has several high-energy interaction models incorporated, including QGSJET, VENUS, and SIBYLL. Thanks to the large number of shower observables at KASCADE, tests of these interaction models have become feasible. Particularly sensitive for such tests are hadrons [5]. For that purpose, the shower simulation is followed by a detailed detector simulation with GEANT. Distributions of measured observables can then be compared to those of simulations.

A complication arises from the fact that the cosmic ray mass composition is not a-priori known. As a solid constraint, measured distributions should always be found between those simulated for proton and iron primaries. Fortunately, some observables are rather mass-insensitive but sensitive to interaction model details, while others apparently are less sensitive to models but rather sensitive to the masses of primary cosmic rays (see Section 5). In fact, many composition-insensitive distributions are reproduced remarkably well by all three models.

Among the models mentioned, the SIBYLL model (version 1.6) is known to generate too few muons. Since muon numbers, like $N_\mu^{\rm tr}$, are the best single energy estimator and therefore KASCADE data usually binned in terms of $N_\mu^{\rm tr}$, SIBYLL performs rather badly in such comparisons [5]. Measured data either match pure iron with SIBYLL or can be even found outside of the predicted proton-to-iron range. When showers are classified in terms of electron number N_e, SIBYLL performs somewhat better but VENUS then fails to match measured relations, like the average hadron shower size N_{H} versus N_e. As a result of these tests, QGSJET shows the best overall agreement with experimental data. At energies beyond the knee even QGSJET shows disagreement in some observables (see Figure 3). Improvement of the interaction models available with CORSIKA is, therefore, a continuing process.

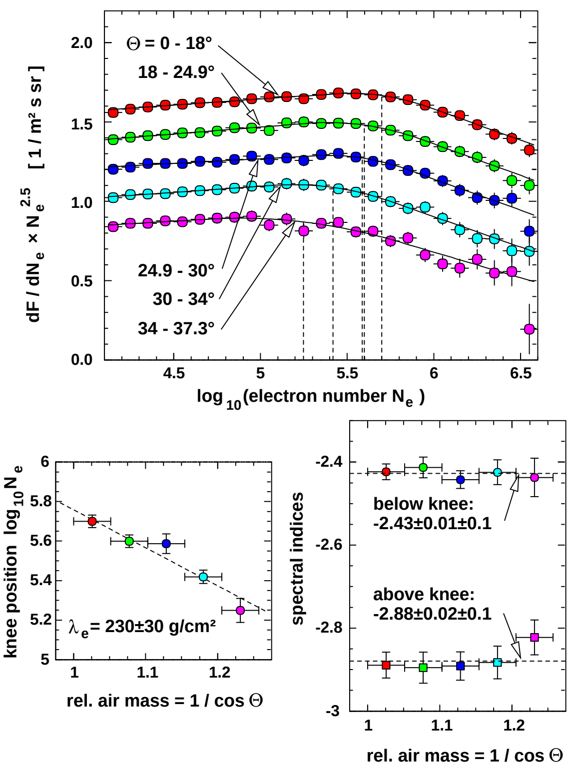

Figure 4. The electron shower size flux spectra (scaled with $N_e^{2.5}$) for different zenith angles (top). Slopes below and above the knee are independent of zenith angle (bottom right) and showers are attenuated as expected with increasing air mass (bottom left).

4. Shower size spectra

The energy spectrum of cosmic rays is rather well described by a power law – with almost the same exponent over more than ten orders of magnitude in energy. The most obvious deviation from a simple power low is the *knee* at an energy of several PeV which was already seen in N_e shower size spectra in the late 1950s. In the meantime the knee has not only been seen in electrons but also in essentially all other shower components, i.e. muons, hadrons, and Cherenkov light. KASCADE has studied electron and muon shower size spectra in great detail and has been the first experiment to see also the knee in hadron size spectra [6,7].

Detection of the knee consistently in different shower components is important for establishing that the knee is, in fact, due to an astrophysical change in the spectrum of cosmic rays and not due to sudden changes in interaction cross sections just beyond present collider energies. An important test for that purpose is also the attenuation of air showers as they pass through different amounts of air (*air mass*), i.e. under different zenith angles. Figure 4 shows that the measured power law exponents below and above the knee are independent of zenith angle and that the attenuation length remains the same below and above the knee. This is consistent with similar results of the EAS-TOP collaboration [8].

For the muon size spectra, a similar pictures results although the muons are less attenuated by the atmosphere and the change of slope at the knee is smaller, due to changes in cosmic ray composition (see Section 5). With a composition as inferred, the hadron size spectrum and its knee is also consistent with the overall spectrum of cosmic rays.

5. Cosmic ray composition

Most previous attempts to infer the composition of cosmic rays by EAS techniques used a single composition-sensitive observable. KASCADE has the advantage of having several observables at hand – which has the inevitable draw-

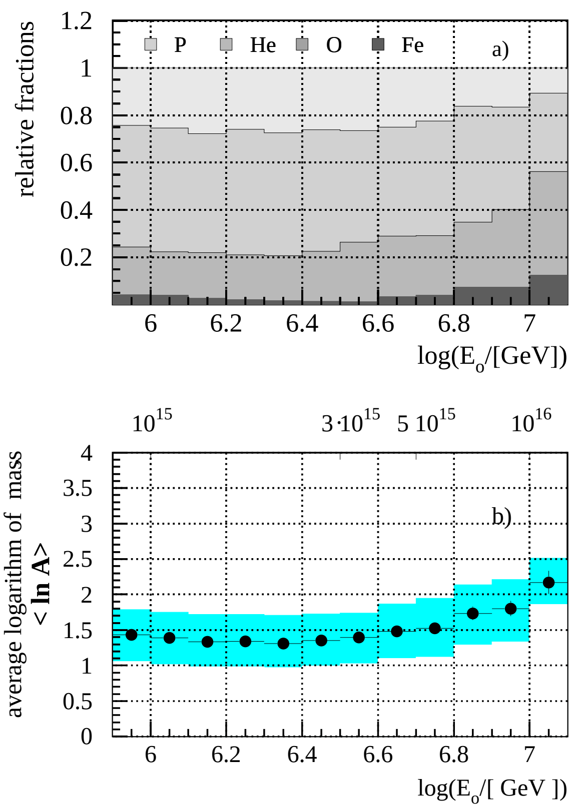

Figure 5. Fractions of four elements (protons, He, O, and Fe; the latter two representing all medium and heavy elements, respectively) from fits of simulated distribution functions of $\log_{10} N_\mu^{\mathrm{tr}} / \log_{10} N_e$ to experimental distributions, as described in the text (a) and resulting average of logarithm of mass numbers (b). The shaded band in b) represents the systematic error due to the use of analytical distribution functions (which in turn were fitted to simulations of limited statistics). Note that the knee is at $\log_{10}(E_0/\mathrm{GeV}) \approx 6.6$.

back of a more complicated analysis. The complication, however, has the benefit that many systematic problems can be studied which otherwise might have gone undetected. A diversity in the analysis is introduced by the fact that showers with cores in the central detector can be studied very well but these account only for a small fraction of all showers recorded with the array.

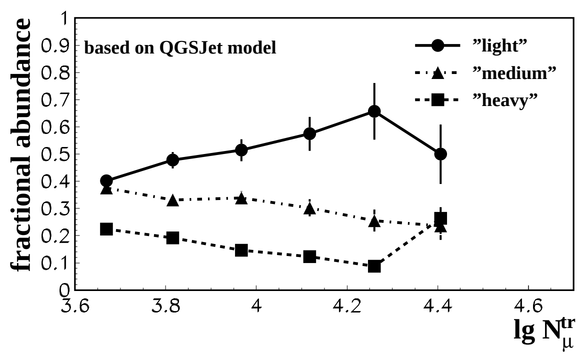

Figure 6. Fractions of three groups of elements from a neural net analysis of MWPC data as well as N_e. Note that the knee is at $\lg N_\mu^{\mathrm{tr}} \approx 4.2$ for almost vertical showers.

For the array the most sensitive observable is the ratio of muon numbers to electron numbers N_μ^{tr}/N_e. This ratio changes with energy simply because the number of electrons – which are heavily attenuated in the atmosphere – is rising faster with energy than the number of muons as the atmospheric depth of the shower maximum increases. A less changing number actually turned out to be, at least in our case, the ratio of logarithms $\log_{10} N_\mu^{\mathrm{tr}} / \log_{10} N_e$. Experimental distributions of that, for different intervals of estimated energies, can be fitted by functions (Gaussians at present) which in turn were fitted to distributions for simulated showers. Central values and widths of these functions for a number of different elements for the cosmic ray primary particle and different energy intervals are fixed by the simulation. Only the relative amounts of the individual elements are free in the composition fit. Results of this approach [9] are shown in Figure 5. There is apparently little change in the composition below the knee and a slow increase of heavy elements above the knee.

For the showers with cores in the central detector, many other composition-sensitive observables can be used. Muons in the MWPCs, for example, show a steeper lateral distribution and a more irregular pattern for showers initiated by protons than for those initiated by iron nuclei. These patterns have been transformed into multifractal dimensions D_6 and D_{-6} which, together with the number of muons in the MWPCs $N_\mu^\star$, electron size N_e and zenith angle θ were fed into neural nets trained with simulated showers of either 2, 3, or 5 elements. Results of this analysis [10] are quite compatible with the N_e-$N_\mu^{\rm tr}$ analysis but show a slightly larger fraction of heavy elements well below the knee and an indication of $\langle \ln A \rangle$ slowly falling with increasing energy below the knee (see Figure 6). In both cases a rising $\langle \ln A \rangle$ is seen above the knee.

A similar result [11] as for the MWPCs is also obtained by applying Bayesian and neural net methods to $N_\mu^{\rm tr}$, N_e, $N_\mu^\star$, and the sum of hadronic energy in the central calorimeter $\sum E_{\rm H}$ to classify individual showers into several mass groups, later correcting for known fractions of misclassified events.

A slightly different picture emerges from analysing average shower observables measured with the hadron calorimeter only [12]. This line of analysis makes use of the fact that these observables – as most EAS observables – are, for single primary mass A, an almost linear function of $\ln A$. Extreme values expected are obtained from simulations for pure protons and pure iron, respectively. For each average observable a mass-sensitive parameter λ is defined such that $\lambda = 0$ for measured data matching simulated protons and $\lambda = 1$ for data matching iron. The physical region is between 0 and 1. For pure elements $\lambda \approx \ln A / \ln 56$. For mixed compositions, different observables may have a different bias towards either of the extremes (i.e. λ is not necessarily equal to $\langle \ln A \rangle / \ln 56$), but in any case are sensitive to changes of the composition. Results for six different observables indicate a rising fraction of heavy elements with rising energy – slowly rising already below the knee.

The differences between these separate lines of analysis are presumably due to systematics in interaction models which affect different shower components in different ways. As already outlined in Section 3, available interaction models describe most data quite well but no model is in perfect agreement for all observables. Until remaining systematics are resolved, slightly different compositions or $\langle \ln A \rangle$ will likely remain when analysing different shower components. At the knee, the different KASCADE methods yield results in the range $1.5 \leq \langle \ln A \rangle \leq 2.8$. Changes of the composition below the knee – if real – are rather small and above the knee there is an unequivocal but not sudden rise of the fraction of heavy elements.

6. All-particle energy spectrum

Although $N_\mu^{\rm tr}$ alone is a rather good estimator of primary energy, a still better estimate is obtained by a combination of $N_\mu^{\rm tr}$ and N_e. The resulting energy spectrum is only weakly depending on the assumed composition. This can be improved further by taking the measured composition into account or fitting, for example, a 2-component flux model (e.g. protons and iron), to measured N_e and $N_\mu^{\rm tr}$ spectra simultaneously. In doing so, unfolding of fluctuations on the steep power-law spectrum – both shower-intrinsic and experimental sampling fluctuations – is important. Otherwise, the real flux would be overestimated.

Following this approach both electron and muon size spectra are reproduced very well with model spectra where only protons have a knee in the energy range used for the fit (about $5 \cdot 10^{14}$–10^{17} eV for N_e and about 10^{15}–$3 \cdot 10^{16}$ eV for $N_\mu^{\rm tr}$). The resulting spectrum (with model spectra extrapolated outside the fitting regions) is illustrated in Figure 7. A similar picture is obtained when drawing separate flux spectra for the light (p+He) and heavy (O+Fe) components from the composition analysis [9]. The knee in the cosmic ray spectrum – in particular as seen in N_e spectra – may in fact be a knee of the light elements only.

7. Conclusions

The KASCADE array has started data taking in 1996. Although not all of the components of the KASCADE experiment are fully completed

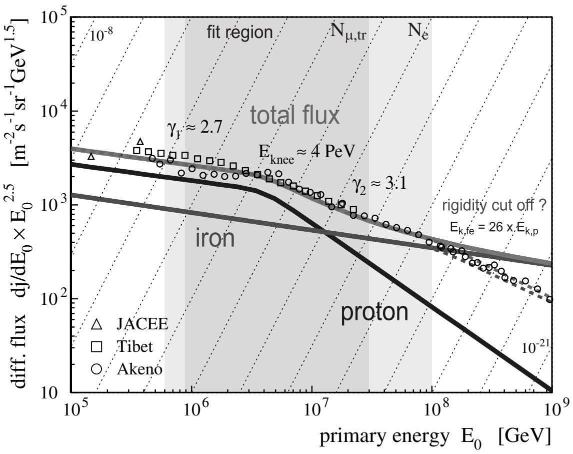

Figure 7. Model energy spectrum (with proton and iron primaries only) simultaneously fitted to electron and muon size spectra, with fluctuations unfolded. Actual fitting regions are indicated by the shaded areas. To have the spectrum in agreement with data from other experiments beyond 10^{17} eV (which are shown as the symbols), an 'iron knee' near 10^{17} eV would be required.

at this time, important result on our view of cosmic rays have started to emerge. Thanks to the many air shower observables available with KASCADE, we are in a situation where detailed tests of interaction models have become feasible. These tests are complementary to present accelerator experiments because they are most sensitive to the behaviour in the forward region. The KASCADE collaboration is actively working on further model improvements with the authors of interaction models suited for EAS simulations.

The array electron and muon shower size spectra have already been measured in great detail, with the shape of the knee and its zenith angle dependence being perfectly consistent with an astrophysical origin of the knee. The knee has, for the first time, also been seen in the hadron size spectrum.

The analysis of the cosmic ray composition is still affected by systematic uncertainties in interaction models, despite important improvements achieved in the last few years. This shows up by a systematically heavier composition seen with hadronic observables than with electrons and muons. Despite remaining systematic uncertainties, a picture has emerged with little changes of the composition below the knee energy and an increasing fraction of heavy elements above the knee. The array data, in particular, are quite consistent with the knee at an energy of about 4 PeV being only a knee in the light elements. At this stage, the data are also consistent with the assumption that each element has a knee at the same rigidity. If protons have the knee at 4 PeV, the knee for iron group elements would be expected at 100 PeV (10^{17} eV). Nevertheless, the real picture may be more complicated than in a minimal model where each element's spectrum has the same change of slope at the same rigidity.

REFERENCES

1. P. Doll et al., Technical Report KfK–4686, Kernforschungszentrum Karlsruhe, 1990.
2. H. O. Klages et al., Nucl. Phys. B, Proc. Suppl. 52B (1997) 92.
3. D. Heck et al., Technical Report FZKA 6019, Forschungszentrum Karlsruhe, 1998.
4. J. Engler et al., Nucl. Instr. & Meth. A 427 (1999) 528.
5. T. Antoni et al., *Tests of high-energy interaction models using the hadronic core of EAS*, submitted to J. Phys. G. (1999)
6. T. Antoni et al., *First observation of the knee in the hadronic component of EAS*, submitted to Astropart. Phys.
7. J. R Hörandel et al., Proc. 26th ICRC, Salt Lake City (1999), paper HE 2.2.41.
8. M. Aglietta et al., Astropart. Phys. 10 (1999) 1.
9. J. Weber et al., Proc. 26th ICRC, Salt Lake City (1999), paper HE 2.2.42.
10. A. Haungs et al., Proc. 26th ICRC, Salt Lake City (1999), paper HE 2.2.39.
11. M. Roth et al., Proc. 26th ICRC, Salt Lake City (1999), paper HE 2.2.40.
12. J. R. Hörandel et al., Proc. 26th ICRC, Salt Lake City (1999), paper HE 2.2.44.